A SA-CASSCF and MS-CASPT2 study on the electronic structure of nitrosobenzene and its relation to its dissociation dynamics

Juan Soto,[1,*] Daniel Peláez[2] and Juan C. Otero[1]

[1]Department of Physical Chemistry
Faculty of Science, University of Málaga, Andalucía Tech., E-29071 Málaga, Spain
[2]Institut des Sciences Moléculaires d'Orsay (ISMO) - UMR 8214.
Université Paris-Saclay, 91405 Orsay Cedex
Corresponding author: soto@uma.es

ABSTRACT

The photodissociation channels of nitrosobenzene (PhNO) induced by a 255 nm photolytic wavelength have been studied with the complete active space self-consistent (CASSCF) method and the multistate second-order multiconfigurational perturbation theory (MS-CASPT2). It is found that there exists a triplet route for photodissociation of the molecule. The reaction mechanism consists on a complex cascade of nonadiabatic electronic transitions involving triple and double conical intersections as well as intersystem crossing. Several of the relevant states (S_2, S_4, and S_5 states) correspond to double excitations. It is worthy to note that the last step of the photodissociation implies an internal conversion process. The experimentally observed velocity pattern of the NO fragment is a signature of such a conical intersection.

I. INTRODUCTION

Nitrosobenzene (C_6H_5NO) is the smallest member of the aromatic C-nitroso family of compounds. This class of compounds presents a rich chemistry[1] as they are involved in many interesting processes in biological processes, organic synthesis, decomposition of energetic materials, or combustion chemistry.[2-5] The underlying reason for such a varied chemistry lies in its rich electronic structure, which has motived its extensive study.[6] From an experimental perspective, its photodissociation dynamics has been studied at various excitation wavelengths using different experimental techniques (see Table I).[5-14]

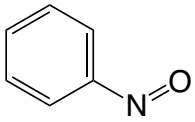

(**Nitrosobenzene**)

The UV absorption spectrum of the molecule in the vapor phase shows a weak absorption band[7,15] with a maximum near 13 333 cm^{-1} (1. 65 eV) together with three strong bands with maxima at 34 500 (4.28), 37 000 (4.59), and 46 500 cm^{-1} (5.77 eV).[12] These features have been assigned to excitations from the ground state to the first four singlet excited states of the molecule. With respect to the photoproducts, there is consensus in that the only possible reaction channel is the Ph-NO bond breaking, *i. e.* $C_6H_5NO \rightarrow C_6H_5 + NO$, independently of the excitation energy. Only at the shortest wavelength used in the experiments[5] (193 nm), an additional reaction product is observed, benzyne (C_6H_4), which arises from the subsequent decomposition of phenyl radical (C_6H_5) generated in the first dissociation step into C_6H_4 and H atom.[5] A remarkable feature in this system is the large energy gap between the S_1 state and its upper neighboring states despite of which, no fluorescence from S_n to S_1 has been observed.[6-9] This is a relevant aspect since it provides a first hint on the photobehavior of nitrosobenzene: its photodissociation takes place on the S_0 or S_1 states. Experiments suggest that after excitation to S_n ($n \geq 2$), the molecule undergoes internal conversion to the S_1 state, in accordance with the absence of observed fluorescence. [6-8] Furthermore, velocity mapping ion imaging data[6-9] suggests that the nascent NO is generated with a propeller-like motion. Indeed, there is direct evidence that NO does have a preferred parallel arrangement of the velocity and angular momentum vectors (**v** || **j**) in the recoil trajectory, which, in turn, supports the hypothesis that deactivation of molecule occurs via internal conversion.[6-9]

Concerning theoretical studies, to the best of our knowledge, nitrosobenzene has not been much studied in contrast to its aliphatic C-nitroso (R-NO) and nitrites (RO-NO) counterparts.[16-21] In this respect, multiconfiguration self-consistent field (MCSCF) approaches are arguably the most appropriate quantum chemical approximations to understand the chemistry of these strongly correlated systems.[22-24] This issue is especially relevant in the case of nitrosobenzene where double excitations, multiple coupled excited states and surface crossings are involved. The objective of this work is precisely disentangle the electronic structure and photodissociation dynamics of the title molecule and for this we will make use of second-order perturbation theory on a MCSCF reference wavefunction.

Table I. Observed products and detection techniques in the photodissociation of nitrosobenzene.

λ_{exc} /nm; [eV]	Observed Products	Detection Technique[a]	Reference
248; [5.00]	C_6H_5 + NO	MII	[5]
193; [6.42]	C_6H_5 + NO // C_6H_4 + H	MII	[5]
305; [4.07]	C_6H_5 + NO	REMPI/VIP	[6]
255; [4.86]	C_6H_5 + NO	LIF	[7]
290; [4.28]	C_6H_5 + NO	REMPI/VIP	[8,12]
266; [4.66]	C_6H_5 + NO	REMPI/VIP	[8,12]
225; [5.51]	C_6H_5 + NO	REMPI	[11]
266; [4.66]	C_6H_5 + NO	TOFMS	[13]
266; [4.66]	C_6H_5 + NO	LIF	[14]

[a]MII: Multimass ion imaging; REMPI: resonance enhanced multiphoton ionization; VIP: velocity-mapped ion imaging; LIF: laser induced fluorescence; TOFMS: time of flight mass spectrometry.

II. METHODS OF CALCULATION

Extended relativistic basis sets of the atomic natural orbital (ANO)-type, the so-called ANO-RCC basis sets[25,26] have been used throughout this work by applying the (C,N,O)[4*s*3*p*2*d*1*f*]/(H)[3*s*2*p*1*d*] contraction scheme. The complete active space self-consistent field (CASSCF)[27-33] and the multi-state second-order perturbation (MS-CASPT2)[34,35] methods have been applied as implemented in the MOLCAS 8.4 program.[36,37] MS-CASPT2 energies have been calculated for the CASSCF-optimized geometries. To avoid the inclusion of intruder states in such calculations an imaginary shift set to 0.1 has been applied. Equally, the IPEA empirical correction has been fixed at 0.25 in all of the calculations. When CASSCF has been applied with the state average approximation, the notation SA*n*-CASSCF has been used, where *n* denotes the number of states of a given symmetry included in the calculation. Minimum energy crossing points of the same spin multiplicity, (i. e. conical intersections) have been optimized with the algorithm[38] implemented in MOLCAS. The analysis of molecular geometries and molecular orbitals have been performed with the programs Gabedit[39] and Molden,[40] while the analysis of vibrational normal modes and vectors defining the branching space (energy difference and derivative coupling) has been performed with the program MacMolplt.[41] Spin-orbit coupling constants have been computed with a spin-orbit Fock-type Hamiltonian.[42-44] For the sake the clarity, two conventions have been used to label

the electronic states: (i) spectroscopic; and (ii) energetic ordering (S_0, S_1,…; T_0, T_1,…). Construction of the potential energy curves (PECs) has been done with our linear interpolation method[45-51] using the full space of non-redundant internal coordinates. The latter provide an accurate 1D-representation of the potential energy surface in the space spanned by a given set of internal coordinates. The PECs for the dissociation are built as follows. First, a common set of 3*N*-6 internal coordinates is defined for the target geometries, the reactant ($\mathbf{R}_1$) and the dissociation fragments separated by a physically reasonable distance ($\mathbf{R}_2$). Our experience shows that a separation distance of 4.7 Å of the dissociative bond (C-N distance for dissociation of nitrosobenzene into phenyl and NO) is enough to reach the asymptotic limit of the PEC of interest. Second, difference between $\mathbf{R}_2$ and $\mathbf{R}_1$ yields an interpolation vector ($\Delta\mathbf{R}$) that connects reactants and products. Third, $\Delta\mathbf{R}$ is divided by *n* (an entire number at the choice of the user). Each of the divisions constitutes what we will call a *step*. In consequence, each step *m* corresponds to a nuclear configuration given by $\mathbf{R}_m = \mathbf{R}_1 + (m/n)\,\Delta\mathbf{R}$. Since we are using internal coordinates (internuclear distances, valence bond and dihedral angles), we cannot give a unique unit for the reaction coordinate. in what follows we will indicate *arbitrary units*. Linear interpolations in internal coordinates present two favorable characteristics: (i) is less demanding computationally than a scan with relaxation of geometry; (ii) all the points along the interpolation vector (reaction coordinate) are necessarily in a straight line. That is not true, however, of scanning of the potential energy surfaces with geometry relaxation.

III. RESULTS AND DISCUSSION

1. Electronic structure of nitrosobenzene and excited states

As is well known, the choice of the different orbital subspaces leading to the definition of a CASSCF wavefunction is crucial to give a correct answer to the problem under study. Otherwise, the conclusions will be unfortunately erroneous.[52-54] In spite of methods for the automated selection of the active space such as the novel AVAS,[55] this task requires some chemical intuition combined with a trial and error process to select the appropriate active orbitals.[22,23] This is particularly true when the process under scrutiny requires the sampling of quite different regions of configuration space (e.g. asymptotic channels where several states converge). Concerning the title molecule, after consideration of the targeted processes, we have chosen an active space consisting in eighteen electrons distributed in fifteen orbitals, hereafter represented as (18e, 15o; Fig. 1). As a first stage,

we have calculated the vertical excitation energies of the molecule at the MS-CASPT2 level using a SA6-CASSCF(18e, 15o) reference wavefunction. Provided that the geometry of the electronic ground state of nitrosobenzene has been experimentally determined to be planar (C_s symmetry),[56,57] these SA-CASSCF calculations have been performed under such a symmetry point group, unless otherwise indicated. Geometries have been also enforced to remain C_s. The results of such vertical excitations are collected in Table II together with the experimental vacuum ultraviolet absorption maxima registered in vapor phase.[7,58] Overall, we observe quite a satisfactory agreement between the present results and experiments, both in energies and intensities. Of course, it should be understood that this comparison is not straightforward given that the computed transitions are not corrected by the zero-point energy of the two states involved in the transition. As first important result, we are able to reproduce the large gap (>2.5 eV) responsible for the absence of fluorescence from S_n to S_1. Moreover, calculated values of oscillator strengths and electronic transitions are consistent with the experimental observation that photolysis at 255 nm (4.86 eV) produces the largest absolute yield of NO fragments,[7] that is, the estimated oscillator strength of the S_6 state yields the highest calculated value among all the studied states. Finally, we remark that S_2 ($1^1A' \rightarrow 2^1A'$), S_4 ($1^1A' \rightarrow 2^1A''$) and S_5 ($1^1A' \rightarrow 3^1A''$) states possess a double-excitation character.

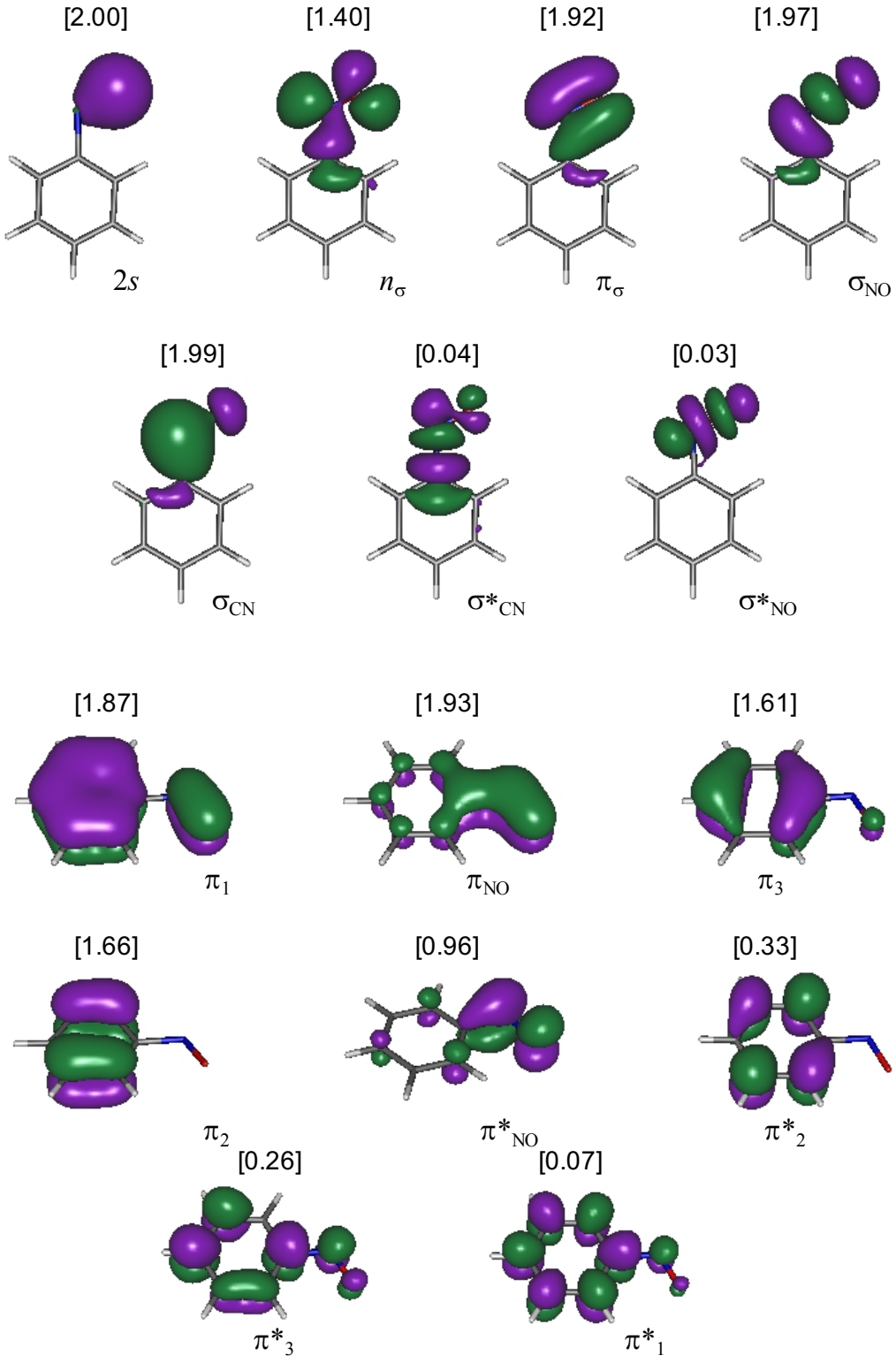

FIG 1. SA6-CASSCF/ANO-RCC natural orbitals included in the active space (18e, 15o) of nitrosobenzene. In square brackets: mean occupation numbers.

Table II. MS-CASPT2 vertical excitation energies of the lowest-lying singlet and triplet states of nitrosobenzene (C_s).[a]

VT[b]	ΔE(eV)[c]	ΔE(eV)[d]	AbM[e]	AbM[f]	$\mathbf{f}_{OSC}$[g]	*Character*[h]	*W*[i]
$1^1A''$	1.67	1.60	1.63*		4.15 10^{-4}	$(n_\sigma)^1(\pi^*_{NO})^1$	77
$2^1A'$	4.27	4.18	4.20	4.22	4.26 10^{-3}	$(n_\sigma)^0(\pi^*_{NO})^2$	69
$3^1A'$	4.45	4.37	4.59	4.58	1.67 10^{-2}	$(\pi_2)^1(\pi^*_{NO})^1$	51
$2^1A''$	4.52	4.38			1.40 10^{-3}	$(n_\sigma)^1(\pi_3)^1(\pi^*_{NO})^2$	29
						$(n_\sigma)^1(\pi^*_3)^1$	28
$3^1A''$	4.69	4.49			8.04 10^{-5}	$(n_\sigma)^1(\pi_2)^1(\pi^*_{NO})^2$	19
						$(n_\sigma)^1(\pi^*_2)^1$	35
$4^1A'$	4.80	4.62	4.75	4.73	2.06 10^{-1}	$(\pi_3)^1(\pi^*_{NO})^1$	75
$4^1A''$	5.63	5.32			-	$(n_\sigma)^1(\pi^*_{NO})^2(\pi_2)^1(\pi^*_{NO})^1(\pi^*_2)^1$	37
$5^1A''$	6.17	5.96	5.88	5.83	1.99 10^{-3}	$(\pi_\sigma)^1(\pi^*_{NO})^1$	46
$5^1A'$	6.23	6.35	6.39*		5.13 10^{-2}	$(\pi_3)^1(\pi^*_2)^1$	23
						$(\pi_2)^1(\pi^*_3)^1$	22
$6^1A''$	6.62	6.85			2.27 10^{-4}	$(n_\sigma)^1(\pi_3)^1(\pi^*_{NO})^1(\pi^*_2)^1$	26
						$(n_\sigma)^1(\pi_2)^1(\pi^*_{NO})^1(\pi^*_3)^1$	16
$6^1A'$	7.13	6.85	7.12*		1.85 10^{-2}	$(\pi_1)^1(\pi^*_{NO})^1$	27

[a]Reference wave function: C_s SA6-CASSCF(18e, 15o)/ANO-RCC; IPEA=0.25. Imaginary shift = 0.1. [b]Vertical transition from the $S_0(1^1A')$ state. [c]CASSCF optimized geometry (C_s). [d]MP2/def2-TZVPP optimized geometry (C_s). [e]UV absorption maxima in vapor phase from Ref. 58, * represents in *n*-hepatane. [f]UV absorption maxima in vapor phase from Ref. 7. [g]Oscillator strength. [h]MS-CASPT2 main electronic configurations of the excited states referred to the ground state configuration (see text). [i]Weight of the configuration in %. Only contributions greater than 15% are included; [reference configuration: $(2s(O))^2(n_\sigma)^2(\pi_1)^2(\pi_2)^2(\pi_3)^2(\pi_\sigma)^2(\sigma_{NO})^2(\sigma_{CN})^2(\sigma_{NO})^2||(\pi^*_1)^0(\pi^*_2)^0(\pi^*_3)^0(\sigma^*_{NO})^0(\sigma^*_{CN})^0(\sigma^*_{NO})^0$].

2. Excitation of nitrosobenzene at 255 nm: Photodissociation into phenyl radical and nitric oxide.

In the following, we will present and discuss our theoretical results regarding the photolysis of nitrosobenzene and compare them to the different experimental results available.[5-14] As starting point to analyze the photodissociation dynamics of this molecule, we consider the potential energy curves depicted in Fig. SI. These linear interpolations, computed at the MS-CASPT2 level of theory with a SA6-CASSCF(16e, 14o) reference wavefunction (C_s symmetry), depict the dissociation of the parent molecule into phenyl radical and nitric oxide on the lowest-lying singlet and triplet potential energy surfaces. It should be highlighted that for their computation, we have omitted the 2*s*(O) orbital from the active space. The initial geometry of the interpolations corresponds to the ground state of nitrosobenzene (**M0**, Fig. 2a) and the end point to the dissociated fragments in their respective ground states (phenyl and nitric oxide). As a

proof of the accuracy of the method, we have calculated the enthalpy of the dissociation reaction at 0 K (by using the CASSCF frequencies of all species for the ZPE correction and the electronic energy at the end point of the interpolation), its magnitude amounts to 2.32 eV, a value that compares quite well with the enthalpy of the reaction at 0 K from Active Thermochemical Tables[59-61] (2.33 ± 0.02 eV).

As first remark, we observe that population of the S_n (n=2-5) excited states cannot lead to direct NO elimination since the dissociation limit of each of these singlet states lies well above the respective vertical excitation energy (Table SI). We also observe the large energy gap between the S_1 state and the upper excited states is well preserved along the dissociation path (Fig. SI). The calculated energy difference between the minima on the first two singlet excited states (**M1**(S_1) and **M2**(S_2) in Fig. 2b and 2c, respectively) is ~1.5 eV. Given the absence of $S_n \rightarrow S_1$ fluorescence as well as the energetic hindrance to direct NO dissociation inferred from the potential energy curves of Fig. SI, we have searched for minimum energy crossing surfaces (conical intersections and intersystem crossings). As guess geometries we have used the structures in the vicinity of the crossings revealed by our interpolations. The resulting points are presented in Fig. 2. In view of these results, curves, relative energies and critical points, we can propose a mechanism to explain the photodissociation of nitrosobenzene after excitation up to S_6 (4.86 eV: 255 nm). This process occurs via an electronic cascade of nonadiabatic transitions. The correlation diagram of the states of the reaction is given in Fig. 3. First, the system decays from S_6 to S_4 through a nonadiabatic transition involving a multistate intersection[62-64] (of states 6, 5 4).[65] Second, the S_4 state leads to the S_3 surface by means of another nonradiative mechanism via a S_4/S_3 conical intersection [**CI1**(S_4/S_3), Fig. 2d]. Third, the S_3 decays to S_2 via a third conical intersection [**CI2**(S_3/S_2), Fig. 2e]. As was mentioned before, there is a very large energy gap between the S_2 and S_1 states. Thus, we have searched for an S_2/S_1 minimum energy crossing point which would provide the sought internal conversion without fluorescence emission and eventually to the formation of NO and phenyl on the S_1 surface. After an exhaustive search, we have found such a conical intersection [**CI3**(S_2/S_1), Fig. 2f]. However, the minimum energy crossing point of CI3 is even higher in energy (4.1 eV) than CI1. Therefore, we think that this channel is not very probable. Hence, to explain the dissociation of the molecule after excitation to S_n ($2 \leq n \leq 6$) another path is necessary. The only one that we have found involves a surface crossing between states of different multiplicity, a mechanism common to another family of N-containing aromatic compounds, the phenyl azide derivatives.[66-68] Once the S_2 state

is populated, it experiences an $S_2(^1A')/T_2(^3A'')$ intersystem crossing, whose minimum energy crossing point is displayed in Fig. 2g [**ISC1**(S_2/T_2), with spin-orbit coupling constant = 23.6 cm^{-1}]. Afterwards, the $T_2(^3A'')$ state decays to the $T_1(^3A')$ state via a triplet/triplet internal conversion whose minimum energy crossing point is depicted in Fig. 2h [**CI4** (T_2/T_1)]. At this point, it is important to notice that the derivative coupling vector of CI4 (Fig. 2h) involves a wagging motion of the system with opposite phase for nitrogen and oxygen in combination with a torsional motion of the NO moiety. In Fig. SIV, we compare the torsional normal mode of M0 with the derivative coupling vector of CI4. Thus, we have search for another singular point with a non-planar arrangement of the molecule on the T_1 surface and what we have found is a T_1/T_0 conical intersection [**CI5** (T_1/T_0), Fig. 2i] whose molecular configuration shows a dihedral angle between the NO moiety and the aromatic ring of ~ 115º. The SA4-CASSCF energy profiles that connect CI3 with CI4 are plotted in Fig. SVa. Therefore, accordingly with this result, it can be proposed that once the lowest triplet state T_0 is populated, the system has sufficient accumulated energy to dissociate into phenyl and NO because this surface is reached via a cascade of non-radiative transitions. Fig. SVb represents the potential energy curve of the dissociation process starting at the geometry of the minimum energy triplet state T_0 [**M3**, Fig. 2j]. Given that the molecular configuration of CI5 shows a dihedral angle between the NO moiety and the aromatic ring of ~ 115º and the minimum energy geometry of the electronic state T_0 is planar [**M3**, Fig. 2j], the CC-NO torsional mode is highly excited and will transform into rotational motion of the salient fragment (NO) at the dissociation limit, in accordance with the conclusion obtained by Keßler and co-authors.[7] It must be remarked that ISC1 is very close to CI2 both geometrically and energetically [the distance (in Cartesian coordinates) between the geometries of ISC1 and CI2 is 0.04 Å, and the energy difference between the two crossings is 0.16 eV]. This fact has been shown to increase the efficiency of the intersystem crossing as recently discussed by us[66-68] and reported by the *old masters*.[69-71] To finish this section, for the sake of clarity, it must be noted that all the singular points given in Fig. 2 are out of the interpolation domain represented in Fig. SI. Fig. 3 represents the correlation diagram for the states involved in the photodissocation route.

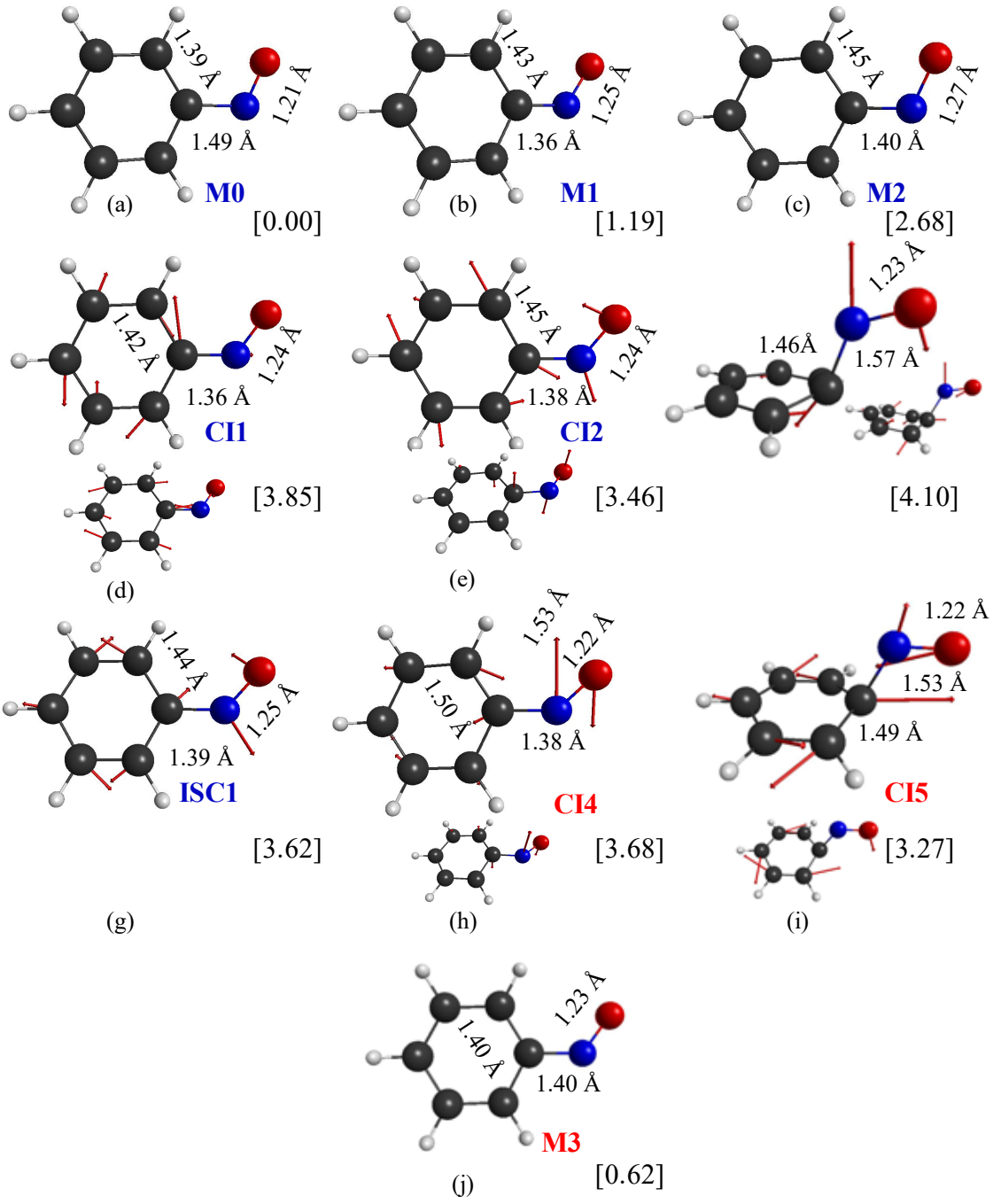

FIG 2. CASSCF/ANO-RCC geometries of the critical points in the photodissociation of nitrosobenzene. (a) **S_0** minimum; (b) **S_1** minimum A"; (c) **S_2** A' minimum; (d) **CI1**(S_4/S_3) conical intersection; (e) **CI2**(S_3/S_2) conical intersection; (f) **CI3**(S_2/S_1) conical intersection; (g) **ISC1**(S_2/T_2) intersystem crossing; (h) **CI4**(T_2/T_1) conical intersection; (i) **CI5**(T_1/T_0) conical intersection; (j) **M3**(T_0) minimum A". Arrows in main figures: gradient difference vector; in small figures: derivative coupling vectors. Cartesian and internal coordinates given in supplementary material. Relative energies (in eV) displayed in brackets.

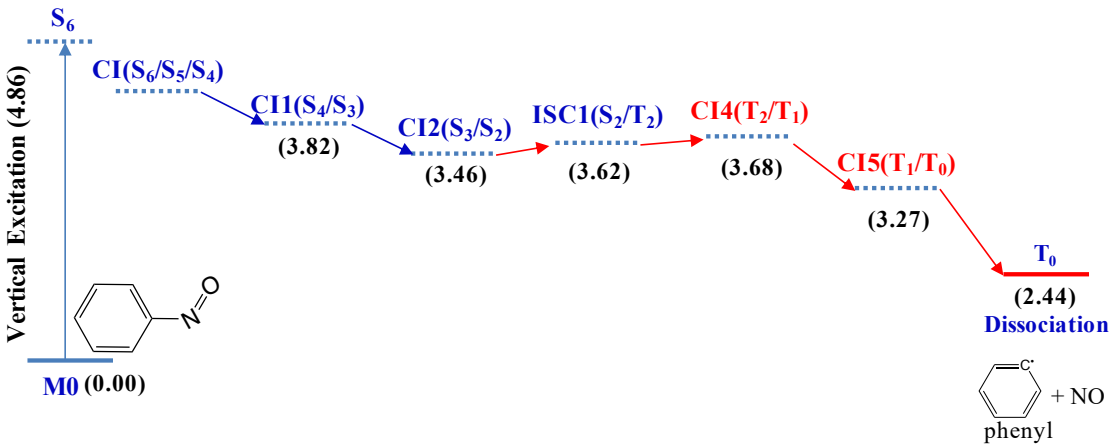

FIG 3. Diagram of correlation of the states involved in the photodissociation of nitrosobenzene. In parenthesis: MS-CASPT2/SA7-CASSCF relative energies in eV.

3. Excitation of nitrosobenzene at 193 nm: Formation of benzyne from phenyl radical.

Benzyne (C_6H_4) is a product observed only when nitrosobenzene is irradiated at 193 nm (6.42 eV). This compound is generated from phenyl radical (C_6H_5) by elimination of atomic hydrogen. It must be noted that the formation of benzyne does not require the absorption of an extra photon by phenyl radical. The available internal energy of the latter, after dissociation from NO, suffices for this.[5] Curiously, although the dissociation-rearrangement channel $C_6H_5NO \rightarrow C_6H_4 + HNO$ is also energetically accessible, after both excitations at 248 nm and 193 nm, no such products were observed by Tseng *et al.*[5]

Fig. 4 represents the potential energy curves corresponding to the lowest-lying doublet states leading to the dissociation of phenyl radical into benzyne and atomic hydrogen. The interpolation curves depicted in Fig. 4 start at the geometry of the minimum energy of the radical [CASSCF(7e, 7o)/ANO-RCC], formed in its doublet ground state (1^2A_1: C_{2v}), and end at the (1^1A_1: C_{2v}) minimum energy of benzyne, with the dissociating hydrogen separated by ~6.7 Å of the aromatic ring. The computed asymptotic limit for the dissociation of C_6H_5 into benzyne and atomic hydrogen in the ground state ($1^2A'$ in Fig. 4) amounts to 3.76 eV. Again, after correcting by the zero-point energy of phenyl and benzyne (by using their respective CASSCF frequencies), we obtain a reaction enthalpy of 3.44 eV, a value that compares quite well with the value at 0 K obtained from Active Thermochemical Tables[59-61] (3.45(7) ± 0.01 eV). This limit is easily accessible for C_6H_5 given that it accumulates around 95% of the available energy (from the exciting photon, 6.42 eV) in its vibrational degrees of freedom, that is, 4.56 eV, after subtraction of translational energy[5] Concerning the possibility of dissociating on the excited states,

two features must be remarked: (i) the next dissociation limit (2^2A' in Fig. 4) is computed almost at the same energy than the excitation of the source, while the other states are even higher in energy than the excitation line; and (ii) almost all the dissociation limits do not reach an asymptotic behavior, that is, they are not dissociative with respect to the formation of benzyne. Therefore, it must be concluded that benzyne is formed from benzyl radical on its lowest potential energy surface (1^2A_1).

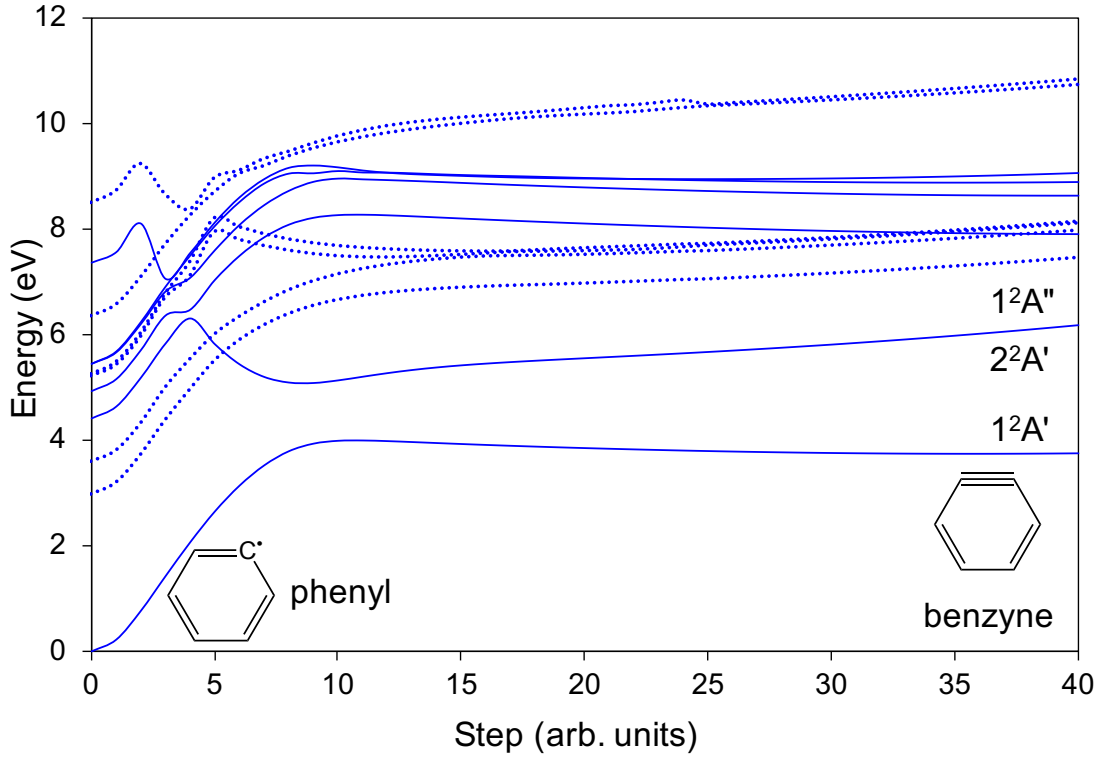

FIG 4. MS-CASPT2/ANO-RCC potential energy curves of the low-lying doublet states of the radical phenyl leading to dissociation into benzyne and atomic hydrogen. Reference wave function: SA6-CASSCF(7e, 7o). A' states (solid lines); A" states (dotted lines).

4. Photodissociation of nitrosobenzene into phenylnitrene and atomic oxygen

In this section, we tackle the study of the elimination of atomic oxygen from nitrosobenzene with the concomitant formation of phenylnitrene. Fig. 5 displays the adiabatic C_s potential energy curves of the low-lying singlet and triplet states for such a reaction. According to the spectroscopic convention, the hierarchy of the energy levels of an atom is *configuration-term-level-state*. The *configuration* of an atom, that is, the orbitals that are occupied by its electrons, is split by electrostatic interactions between electrons into *terms*; due to spin-orbit coupling, these *terms* are separated into *levels*; and,

finally, the interaction of electrons with an external field uncouples these *levels* into *states*. Given that in the calculations of this reaction (Fig. 5), the spin-orbit Hamiltonian is not included, we will consider a *configuration-term-state* hierarchy. In this case, the role of external field over the electrons of each fragment (oxygen and phenylnitrene) is played by the other fragment. Thus, we would observe at the dissociation limit of nitrosobenzene the following almost degenerate states arising from the oxygen atom: three triplet states arising from the O(^{3}P) term, five singlet states from the O(^{1}D) term and one singlet state from O(^{1}S) term. However, as the ground state of phenylnitrene is a triplet[66] (Table SII), the relationships of the states at such dissociation limit are somewhat more cumbersome. For example, the six lowest energy states are almost asymptotically degenerate, because they come from the triplet states of oxygen and the ground state of phenylnitrene, respectively.

Concerning the energetics of the reaction of oxygen extrusion, it must be noted that its lower dissociation limit, despite accessible, is considerably higher in energy ($\underline{\Delta E}$~2.4 eV) than the analogous dissociation limit for the nitric oxide formation channel (Fig. SI). From our point of view, this explains only partially why this reaction channel is not observed experimentally. The most important factor, in our opinion, is the driving force of the cascade of conical intersections after excitation at 255 nm, that guides the system after photon excitation to dissociation into NO and phenyl.

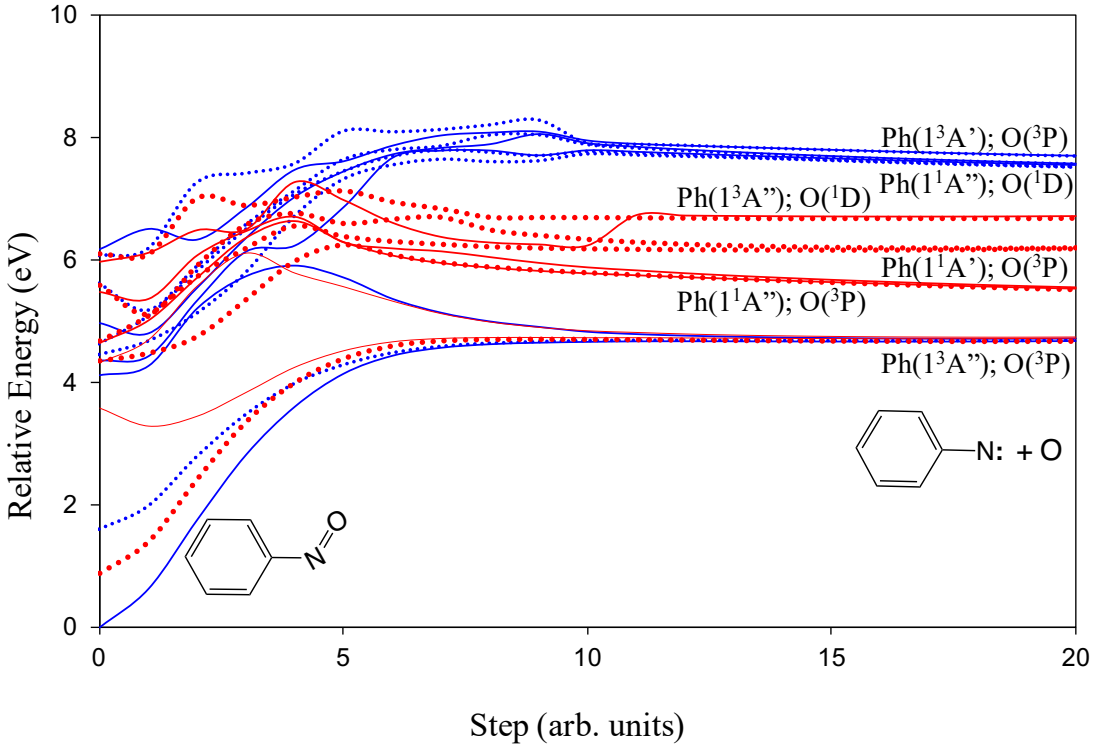

FIG 5. MS-CASPT2/ANO-RCC potential energy curves leading to dissociation of nitrosobenzene into phenylnitrene and atomic oxygen. Reference wave function: SA5-CASSCF(16e, 14o). A' states (solid lines); A"(dotted lines). Singlet (blue lines); triplet (red lines).

IV. CONCLUSIONS

In this work, we propose a reaction mechanism for photodissociation of nitrosobenzene into phenyl and NO that occurs via two different routes, singlet or triplet. In essence, it consists in an electronic cascade of nonadiabatic transitions (triple and double conical intersections plus intersystem crossing) that starts at the S_6 state and ends at the T_0 state.

Our work explains the experimental observations, that is, products and dynamical properties of the products:

(1) The estimated oscillator strength of the S_6 state yields the higher calculated value among all the studied states, which is in accordance with the experimental observation that photolysis at 255 nm produced the largest absolute yield of NO fragments,[7] provided that there only one dissociation channel.

(2) The proposed cascade of nonadiabatic transitions, which dominates the process, is in accordance with the conclusion obtained by Keßler *et al*.,[7] that is, the NO elimination occurs after fast internal conversion (or intersystem crossing) to the triplet state T_0 what induces a highly excited torsional state.

(3) The origin of the torques producing the propellerlike trajectory[6-9] of NO is a signature of the deactivation process associated with the CI5(T_1/T_0) conical intersection (Fig. 2i).

SUPPLEMENTARY MATERIAL

Supplementary material contains energetics of dissociation limits, Cartesian coordinates of all the critical points and vertical excitation energies of phenylnitrene.

ACKNOWLEDGEMENTS

This work has been supported by the Spanish Ministerio de Economía, Industria y Competividad (CTQ2015-65816-R) and projects UMA18-FEDER-JA-049 and P18-RT-4592 of Junta de Andalucía and FEDER founds. The authors thank Rafael Larrosa and Darío Guerrero for the technical support in running the calculations and the SCBI (Supercomputer and Bioinformatics) of the Univ. Málaga for computer and software

resources. DP gratefully acknowledges computational support by Andrei Borissov (ISMO).

DATA AVAILABILITY

The data that supports the findings of this study are available within the article [and its supplementary material].

REFERENCES

[1]H. Yamamoto and N. Momiyama, Chem. Comm. 3514 (2005).
[2]P. Zuman and B. Shah, Chem. Rev. **94**, 1621 (1994).
[3]J. Chen, J. Xiong, Y. Song, Y. Yu, and L. Wu, Appl. Surf. Sci. **440**, 1269 (2018).
[4]D. B. Galloway, J. A. Bartz, L. G. Huey, and F. F. Crim, J. Chem. Phys. **98**, 2107 (1993).
[5]C.-M. Tseng, Y. M. Choi, C.-L. Huang, C.-K. Ni, Y. T. Lee, and M. C. Lin, J. Phys. Chem. A **108**, 7928 (2004).
[6]J. A. Bartz, S. C. Everhart, and J. I. Cline, J. Chem. Phys. **132**, 074310 (2010).
[7]A. Kessler, A. Slenczka, R. Seiler, and B. Dick, Phys. Chem. Chem. Phys. **3**, 2819 (2001).
[8]T. J. Obernhuber, U. Kensy and B. Dick, Phys. Chem. Chem. Phys. **5**, 2799 (2003).
[9]A. Kessler, U. Kensy, and B. Dick, Chem. Phys. Lett. **289**, 516 (1998).
[10]S. Niles and C. A. Wight, Chem. Phys. Lett. **154**, 458 (1989).
[11]R. Seiler and B. Dick, Chem. Phys. **288**, 43 (2003).
[12]J.-H. Huang, G.-J. Wang, X.-B. Gu, K.-L. Han, and G.-Z. He, J. Phys. Chem. A **104**, 10079 (2000).
[13]Y.-M. Li, J.-L. Sun, K.-L. Han, and G.-Z. He, Chem. Phys. Lett. **338**, 297 (2001).
[14]M. R. S. McCoustra and J. Pfab, Chem. Phys. Lett. **122**, 395 (1985).
[15]V. V. Bhujle, C. N. R. Rao, and U. P. Wild, J. Chem. Soc., Faraday Trans. 2 **70**, 1761 (1974).
[16]D. Peláez, J. F. Arenas, J. C. Otero, and J. Soto, J. Chem. Phys. **125**, 164311 (2006).
[17]J. Soto, D. Peláez, J. C. Otero, F. J. Avila, and J. F. Arenas, Phys. Chem. Chem. Phys **11**, 2631 (2009).
[18]D. Peláez, J. F. Arenas, J. C. Otero, and J. Soto, J. Org. Chem. **72**, 4741 (2007).
[19]J. F. Arenas, J. C. Otero, D. Peláez, and J. Soto, J. Org. Chem. **71**, 983 (2006).
[20]C. Ruano, J. C. Otero, J. F. Arenas, and J. Soto, Chem. Phys. Lett. **553**, 17 (2012).
[21]J. F. Arenas, J. C. Otero, D. Peláez, and J. Soto, J. Phys. Chem. A **109**, 7172 (2005).
[22]D. A. Kreplin, P. J. Knowles, and H.-J. Werner, J. Chem. Phys. **150**, 194106 (2019).
[23]D. A. Kreplin, P. J. Knowles, and H.-J. Werner, J. Chem. Phys. **152**, 074102 (2020).
[24]B. Helmich-Paris, J. Chem. Phys. **150,** 174121 (2019).
[25]B. O. Roos, R. Lindh, P.-Å. Malmqvist, V. Veryazov, and P.-O. Widmark, J. Phys. Chem. A **108**, 2851 (2004).
[26]B. O. Roos, R. Lindh, P.-Å. Malmqvist, V. Veryazov and P.-O. Widmark, J. Phys. Chem. A **109**, 6575 (2005).
[27]B. O. Roos, in Advances in Chemical Physics; Ab initio Methods in Quantum Chemistry II, ed. K. P. Lawley, John Wiley & Sons, Chichester, UK, 1987, ch. 69, p. 399.
[28]B. O. Roos, P. R. Taylor, and P. E. M. Siegbahn, Chem. Phys. **48**, 157 (1980).
[29]B. O. Roos, Int. J. Quantum Chem. **18**, 175 (1980).
[30]P. E. M. Siegbahn, J. Almlöf, A. Heiberg, and B. O. Roos, J. Chem. Phys. **74**, 2384 (1981).
[31]H.-J. Werner and W. Meyer, J. Chem. Phys. **73**, 2342 (1980).
[32]H.-J. Werner and W. Meyer, J. Chem. Phys. **74**, 5794 (1981).
[33]J. Olsen, Int. J. Quantum. Chem. **111**, 3267 (2011).

[34]B. O. Roos, K. Andersson, M. P. Fülscher, P. Å. Malmqvist, L. Serrano-Andrés, K. Pierloot, and M. Merchán, Adv. Chem. Phys. **93**, 219 (1996).
[35]J. Finley, P.-Å. Malmqvist, B. O. Roos, and L. Serrano-Andrés, Chem. Phys. Lett. **288**, 299 (1998)
[36]MOLCAS 8.4 V. Veryazov, P.-O. Widmark, L. Serrano-Andrés, R. Lindh, and B. O. Roos, Int. J. Quantum Chem. **100**, 626 (2004).
[37]MOLCAS 8.4 F. Aquilante, J. Autschbach, R. K. Carlson, L. F. Chibotaru, M. G. Delcey, L. De Vico, I. Fdez. Galván, N. Ferré, L. M. Frutos, L. Gagliardi, M. Garavelli, A. Giussani, C. E. Hoyer, G. Li Manni, H. Lischka, D. Ma, P. Å. Malmqvist, T. Müller, A. Nenov, M. Olivucci, T. B. Pedersen, D. Peng, F. Plasser, B. Pritchard, M. Reiher, I. Rivalta, I. Schapiro, J. Segarra-Martí, M. Stenrup, D. G. Truhlar, L. Ungur, A. Valentini, S. Vancoillie, V. Veryazov, V. P. Vysotskiy, O. Weingart, F. Zapata, and R. Lindh, J. Comp. Chem. **37**, 506 (2016).
[38]I. Fdez. Galván, M. G. Delcey, T. B. Pedersen, F. Aquilante, and R. Lindh, J. Chem. Theory Comput. **12**, 3636 (2016).
[39]A. R. Allouche, J. Comput. Chem. **32**, 174 (2011).
[40]G. Schaftenaar and J. H. J. Noordik, J. Comput. Aided Mol. Design. **14**, 123 (2000).
[41]B. M. Bode and M. S. Gordon, J. Mol. Graphics Modell. **16**, 133 (1998).
[42]B. A. Heß, C. M. Marian, U. Wahlgren, and O. Gropen, Chem. Phys. Lett. **251**, 365 (1996).
[43]P. A. Malmqvist, B. O. Roos, and B. Schimmelpfenning, Chem. Phys. Lett. **357**, 230 (2002).
[44]C. Ribbing, B. Gilliams, K. Pierloot, B. O. Roos, and G. Karlström, J. Chem. Phys. **109**, 3145 (1998).
[45]J. F. Arenas, J. C. Otero, D. Peláez, J. Soto, and L. Serrano-Andrés, J. Chem. Phys. **121**, 4127 (2004).
[46]M. Algarra, V. Moreno, J.M. Lázaro-Martinez, E. Rodríguez-Castellón, J. Soto, J. Morales, and A. Benitez, J. Colloid Interface Sci. **561**, 678 (2020).
[47]M. Algarra and J. Soto, ChemPhysChem **21**, 1126 (2020).
[48]M. Algarra, J. Soto, L. Pinto da Silva, M. S. Pino-González, J. R. Rodríguez-Borges, J. Mascetti, F. Borget, A. Reisi-Vanani, and R. Luque, J. Phys. Chem. A **124**, 1911 (2020).
[49]S. Kopec, E. Martínez-Núñez, J. Soto, and D. Peláez, Int. J. Quantum. Chem. **119**, e26008 (2019).
[50]R. L. Panadés-Barrueta, E. Martínez-Núñez, and D. Peláez, Front. Chem. **7**, 516 (2019).
[51]M. Louleb, L. Latrous, A. Rios, M. Zougagh, E. Rodriguez-Castellon, M. Algarra, and J. Soto, ACS Appl. Nano Mater. 3, 8004 (2020).
[52]J. Soto, F. J. Avila, J. C. Otero, and J. F. Arenas, Phys. Chem. Chem. Phys **13**, 7230 (2011).
[53]J. F. Arenas, I. Lopez-Tocon, J. C. Otero, and J. Soto, J. Am. Chem. Soc. **124**, 1728 (2002).
[54]F. Bernardi, M. Olivucci, M. A. Robb, T. Vreven, and J. Soto, J. Org. Chem. **65**, 7847 (2000).
[55]E. R. Sayfutyarova, Q. Sun, G. K.-L. Chan, and G. Knizia, J. Chem. Theory Comput. **13**, 4063 (2017).
[56]Y. Hanyu and J. E. Boggs, J. Chem. Phys. **43**, 3454 (1965).

[57]Y. Hanyu, C. O. Britt, and J. E. Boggs, J. Chem. Phys. **45**, 4725 (1966).
[58]K. Tabei and S. Nagakura, Bull. Chem. Soc. Jpn. **38**, 965 (1965).
[59]B. Ruscic and D. H. Bross, Active Thermochemical Tables (ATcT) values based on ver. 1.122p of the Thermochemical Network (2020); available at ATcT.anl.gov.
[60]B. Ruscic, R. E. Pinzon, M. L. Morton, G. von Laszewski, S. Bittner, S. G. Nijsure, K. A. Amin, M. Minkoff, and A. F. Wagner, J. Phys. Chem. A **108**, 9979 (2004).
[61]B. Ruscic, R. E. Pinzon, G. von Laszewski, D. Kodeboyina, A. Burcat, D. Leahy, D. Montoya, and A. F. Wagner, J. Phys. Conf. Ser. 16, 561 (2005).
[62]S. Matsika and D. R. Yarkony, J. Chem. Phys. **117**, 6907 (2002).
[63]S. Han and D. R. Yarkony, J. Chem. Phys. **119**, 5058 (2003).
[64]S. Han and D. R. Yarkony, J. Chem. Phys. **119**, 11561 (2003).
[65]In spite of an exhaustive search of CI(S_6/S_5) and CI(S_5/S_4) conical intersections, it was impossible to find the minimum energy crossing point on the seam of crossing of the respective conical intersection. Furthermore, the geometrical optimization processes of such crossings show oscillating behaviors of the convergence parameters, being unable to reach the fulfillment of the standard thresholds of convergence because the calculated energies of the S_4, S_5 and S_6 states are almost degenerated.
[66]J. Soto and J. C. Otero, J. Phys. Chem. A **123**, 9053 (2019).
[67]J. Soto, J. C. Otero, F. J. Avila, and D. Peláez, Phys. Chem. Chem. Phys. **21**, 2389 (2019).
[68]D. Aranda, F. J. Avila, I. Lopez-Tocon, J. F. Arenas, J. C. Otero, and J. Soto Phys. Chem. Chem. Phys. **20**, 7764 (2018).
[69]M. Bixon and J. Jortner J. Chem. Phys. **48**, 715 (1968).
[70]S. D. Colson and E. R. Bernstein J. Chem. Phys. **43**, 2661 (1965).
[71]V. Weisskopfand and E. Wigner. Z. Physik. **63**, 54 (1930).